Leveraging Channel Coherence in Long-Term iEEG Data for Seizure Prediction

Sha Lu, Lin Liu, Jiuyong Li, Jordan Chambers, Mark J. Cook, and David B. Grayden

***Abstract*—Epilepsy affects millions worldwide, posing significant challenges due to the erratic and unexpected nature of seizures. Despite advancements, existing seizure prediction techniques remain limited in their ability to forecast seizures with high accuracy, impacting the quality of life for those with epilepsy. This research introduces the Coherence-based Seizure Prediction (CoSP) method, which integrates coherence analysis with deep learning to enhance seizure prediction efficacy. In CoSP, electroencephalography (EEG) recordings are divided into 10-second segments to extract channel pairwise coherence. This coherence data is then used to train a four-layer convolutional neural network to predict the probability of being in a preictal state. The predicted probabilities are then processed to issue seizure warnings. CoSP was evaluated in a pseudo-prospective setting using long-term iEEG data from ten patients in the NeuroVista seizure advisory system. CoSP demonstrated promising predictive performance across a range of preictal intervals (4 to 180 minutes). CoSP achieved a median Seizure Sensitivity (SS) of 0.79, a median false alarm rate of 0.15 per hour, and a median Time in Warning (TiW) of 27%, highlighting its potential for accurate and reliable seizure prediction. Statistical analysis confirmed that CoSP significantly outperformed chance ($p = 0.001$) and other baseline methods ($p < 0.05$) under similar evaluation configurations.**

***Index Terms*—Seizure prediction, seizure forecasting, iEEG, coherence, epilepsy.**

Received 9 July 2024; revised 27 February 2025; accepted 25 March 2025. Date of publication 1 April 2025; date of current version 7 August 2025. This work was supported by the Australian Government through the Australian Research Council's Training Centre in Cognitive Computing for Medical Technologies under project Number ICI70200030. *(Corresponding authors: Sha Lu; Lin Liu; David B. Grayden.)*

This work involved human subjects or animals in its research. The NeuroVista dataset used in the research was collected following ethical approval from the Human Research Ethics Committee at St. Vincent's Hospital, Melbourne under Application No. LRR145/13.

Sha Lu, Lin Liu, and Jiuyong Li are with the STEM, University of South Australia, Adelaide, SA 5001, Australia (e-mail: Sha.Lu@unisa.edu.au; Lin.Liu@unisa.edu.au; Jiuyong.Li@unisa.edu.au).

Jordan Chambers is with the Department of Biomedical Engineering, The University of Melbourne, Melbourne, VIC 3010, Australia (e-mail: jordanc@unimelb.edu.au).

Mark J. Cook and David B. Grayden are with the Department of Biomedical Engineering, The University of Melbourne, Melbourne, VIC 3010, Australia, and also with the Department of Medicine, St. Vincent's Hospital and Graeme Clark Institute, University of Melbourne, Melbourne, VIC 3010, Australia (e-mail: markcook@unimelb.edu.au; grayden@unimelb.edu.au).

Digital Object Identifier 10.1109/JBHI.2025.3556775

I. Introduction

EPILEPSY is a significant neurological disorder characterized by recurrent seizures that can manifest as abnormal movements, behaviors, or altered consciousness, and it affects approximately 50 million people worldwide [32]. The primary approach to managing epilepsy involves the use of anti-epileptic drugs and surgical interventions in selected cases unresponsive to medication. However, about 30% of epilepsy patients do not respond to these treatments, living with seizures refractory to current pharmacological and surgical options [32]. The erratic and often unexpected nature of seizures poses challenges for these patients in maintaining regular daily activities. Recent advancements in computational models, particularly those based on electroencephalography (EEG) data, have shown promise in predicting seizures, potentially enhancing the quality of life for epilepsy patients [11], [21], [32].

EEG is a crucial tool for diagnosing and treating epilepsy [5], [22], [34]. A seizure is characterized by an excessive, hypersynchronous neuronal discharge in the brain, which is often detectable through EEG [40]. There are two primary types of EEG data: scalp EEG and intracranial EEG (iEEG). Scalp EEG, a non-invasive technique, involves placing electrodes on the patient's scalp, making it suitable for broad diagnostic purposes. Conversely, iEEG requires the implantation of electrodes directly onto or within the brain, offering higher resolution signals critical for studying severe refractory epilepsy. Recent technological advances, exemplified by initiatives such as NeuroVista [17] and Epi-Minder [6], are advancing the field through the development of technologies for chronic implantation of electrodes for continuous, ultra-long-term seizure monitoring.

When conducting seizure prediction based on EEG data, traditional approaches often require the manual extraction of features from EEG data before the application of seizure prediction algorithms [15], [22]. This process requires expert knowledge to identify the features to ensure the efficacy and accuracy of predictions [11], [18], [21]. In contrast, deep learning methods provide the advantage of automatically extracting features from EEG recordings [25]. A common deep learning approach is to utilize deep neural network classification models trained through supervised learning. Specifically, EEG recordings are categorized into four phases: preictal (the period shortly before a seizure onset), ictal (during a seizure), postictal (immediately after a seizure), and interictal (the period between seizures) [33]. Seizure prediction can be considered a classification task that

aims to distinguish between the preictal and interictal periods. Various neural network architectures have been explored for seizure prediction, such as convolutional neural network (CNN) [7], [12], [26], long short-term memory (LSTM) network [9], [14], and graph neural network (GNN) [24].

However, most seizure prediction methods utilize short-term EEG data for their analysis, and only a few studies are based on long-term EEG data. Research [13] has highlighted that seizure prediction models trained on time-correlated data from short-term EEG recordings often struggle to generalize to datasets gathered in more prospective, real-world settings. In contrast, long-term EEG data, captured from patients during their daily activities, not only provide a larger volume of data but also exhibit greater variability. This helps mitigate the issue of time-correlation in analyses, presenting a more robust basis for seizure prediction models.

Therefore, this study utilized long-term iEEG data from the NeuroVista dataset [17] to evaluate the effectiveness of the proposed method. Previous research using the NeuroVista dataset has advanced the field by demonstrating the potential of critical slowdown as a biomarker for seizure prediction [16], the informativeness of high-frequency activity to epilepsy [27], [28], and the application of CNNs on wearable devices for seizure prediction [12]. Despite these advancements, there remain significant opportunities for further exploration and development using this dataset.

Research [1], [10], [20], [31] has shown that channel coherence in EEG data is a valuable indicator of epileptic seizures. Coherence in EEG measures the linear dependency between waveform signals across various frequency bands, and it provides insights into how different brain regions function in a coordinated manner or synchronize with each other [30], [38], [41]. Coherence analysis has been used in epilepsy research to gain valuable insights into seizure dynamics [20], [23], detect seizure onset [10], and understand changes in brain connectivity during epileptic seizures [1], [31].

However, no EEG-based seizure prediction method to date has utilized the full channel coherence as a feature. It is a non-trivial task to effectively utilize channel coherence as a feature for seizure prediction. The computation of pairwise coherence across frequencies and time results in intricate, high-dimensional data, posing challenges for traditional seizure prediction methodologies that rely on manual feature extraction. Prior work on coherence analysis tackled this by reducing dimensions either through channel strategies, selecting channel subsets [31], averaging across channels [10], [20], [23], or employing global coherence [1], or frequency approaches, such as narrowing frequency ranges [1], [10], [23] or focusing on key EEG sub-bands [20], [31]. These approaches, however, do not fully leverage the detailed information available in pairwise coherence.

In this paper, we propose to use full pairwise channel coherence as a feature for seizure prediction. The proposed **Co**herence-based **S**eizure **P**rediction (CoSP) method addresses the challenges associated with the high-dimensionality and complexity of pairwise coherence data by leveraging deep learning techniques that excel at extracting meaningful features from intricate datasets. This enables the effective utilization of pairwise coherence for seizure prediction. CoSP has demonstrated promising performance on the NeuroVista dataset across various preictal intervals.

TABLE I
SEIZURE INFORMATION OF THE PATIENTS IN THE STUDY

Patient	#SZ	Days	#SZ-Daily	#Lead-SZ	Included
1	150	767	0.2	90	Yes
2	32	730	0.04	32	Yes
3	390	557	0.7	231	Yes
6	71	441	0.16	56	Yes
8	467	558	0.84	338	Yes
9	204	395	0.52	186	Yes
10	545	373	1.46	216	Yes
11	467	722	0.65	288	Yes
13	500	747	0.67	341	Yes
15	77	466	0.17	75	Yes

#SZ: total number of seizures in trial; **Days**: total days in trial; **#SZ-Daily**: average average daily number of seizures; **#Lead-SZ**: number of lead seizures; **Included**: if included in our experiments.

II. MATERIALS AND METHODS

A. Data Preparation

The NeuroVista dataset [17] comprises iEEG recordings from 15 patients with refractory focal epilepsy. The dataset, approved by the Human Research Ethics Committee of St. Vincent's Hospital, Melbourne (approval LRR145/13), was collected for a clinical feasibility study. The recording duration for each patient ranges from 0.5 to 2.1 years, with an average duration of 520 days across all patients. The recordings were captured using 16 electrodes at a 400 Hz sampling rate. For our experiment, we excluded patients with fewer than 20 lead seizures, specifically patients 4, 5, 12, and 14. Additionally, we excluded patient 7 due to the short recording duration. The total number of seizures and the recording period for each patient are detailed in Table I. More details about the data can be found at [17].

As is common in seizure prediction, we focused only on lead seizures [16], which were defined as seizures occurring without any preceding seizures for at least four hours. To minimize contamination from postictal data, we excluded recordings from the four hours following a seizure. Additionally, the initial 100 days of EEG recordings for each patient were excluded to address inconsistencies caused by device implantation [17]. The remaining recordings were categorized into ictal, postictal, interictal, and preictal phases, as illustrated in Fig. 2. Interictal and preictal recordings were divided into 10-second EEG segments for analysis.

The NeuroVista dataset includes data dropouts lasting from minutes to days across all patients. To maintain data integrity, any 10-second segments with more than 10% data dropouts were excluded. For segments with less than 10% dropouts, missing values were imputed with the median value of the respective channels in that segment. EEG segments were filtered using a low-pass finite impulse response filter with a cutoff frequency of 170 Hz to eliminate a 200 Hz artifact associated with device charging [16].

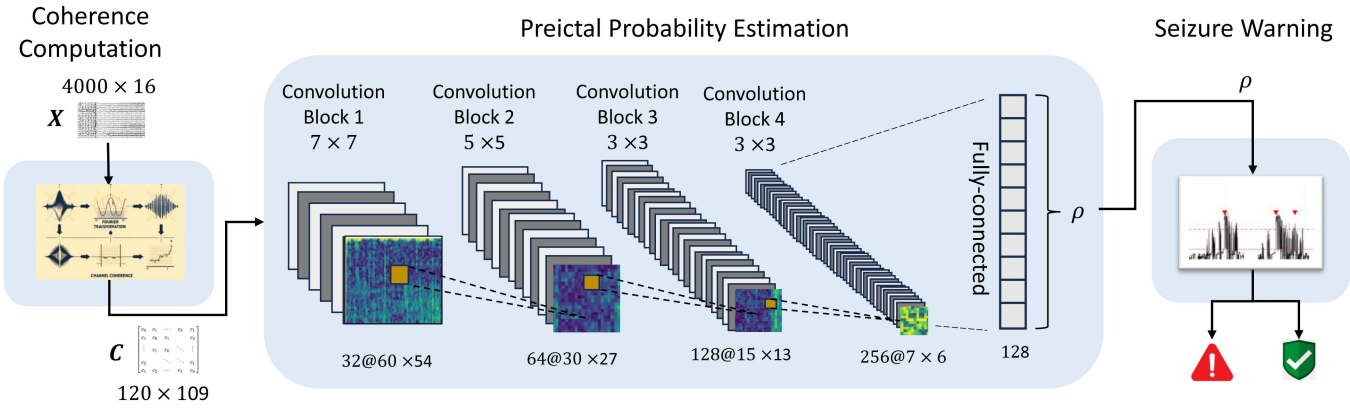

Fig. 1. The framework of the CoSP method. The CoSP method comprises three main modules: coherence computation, preictal probability estimation, and seizure warning. The input EEG segment $\mathbf{X}$ (dimensions 4000×16) is processed into a coherence matrix $\mathbf{C}$ (dimensions 120×109) in the coherence computation module. The coherence matrix $\mathbf{C}$ is then passed through the preictal probability estimation module to yield the estimated preictal probability ρ. The seizure warning module decides whether or not to issue a seizure warning based on ρ.

TABLE II
SEIZURE PREDICTION PERFORMANCE OF COSP

Patient	SOP	Threshold	ROC AUC	SS	FPR/h	TiW	PP
1	15	0.70	0.78	0.92	0.22	25%	0.68
2	90	0.50	0.69	0.80	0.03	18%	0.66
3	45	0.55	0.82	0.91	0.07	29%	0.65
6	4	0.60	0.69	0.63	0.79	29%	0.44
8	15	0.60	0.80	0.79	0.21	28%	0.57
9	60	0.50	0.73	0.92	0.05	25%	0.69
10	180	0.50	0.73	0.77	0.03	35%	0.50
11	4	0.70	0.91	0.71	0.57	12%	0.63
13	4	0.50	0.83	0.79	0.67	16%	0.67
15	45	0.45	0.65	0.75	0.09	33%	0.50
Median			0.76	0.79	0.15	27%	0.64

Subsequently, the EEG segments were divided into training, validation, and test sets based on the lead seizure counts, with recordings from the chronologically first 60% of seizures used for training, the next 20% for validation, and the final 20% for testing. The number of seizures used in the training, validation, and test sets for each patient is detailed in Table II. It is important to note that CoSP was trained using only the training and validation sets, while the test set was employed exclusively for evaluating model performance.

B. The CoSP Method

As shown in Fig. 1, the CoSP method comprises three main modules: coherence computation, preictal probability estimation, and a seizure warning module. In the coherence computation module, a pairwise coherence matrice are computed from each 10-second EEG segment. These matrices are then used as inputs in the preictal probability estimation module, where a CNN predicts the probability of each segment being preictal. Finally, the predicted probabilities are process in the seizure warning module to issue seizure warnings.

1) Coherence Computation: Given an input EEG segment $\mathbf{X} \in \mathbb{R}^{n \times h}$, where n represents the number of time steps and h represents the number of channels, this module computes the pairwise coherence between channels across different frequency bands.

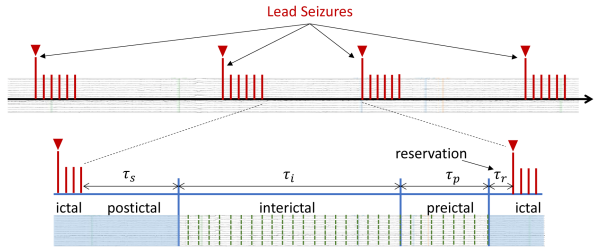

Fig. 2. Schematic of EEG data preparation for our study: continuous EEG recordings are shown as pale traces, with seizures marked by red lines. Our analysis only focused on predicting lead seizures, indicated by longer red lines with inverted triangles. The time between two consecutive seizure clusters was divided into four phases: the postictal period (τ_s, set at 4 hours), the interictal period (τ_i), the preictal period (τ_p), and the prediction reservation time (τ_r, set at 1 minute). For seizure prediction, we utilize only the interictal and preictal data, which were divided into 10-second EEG segments for subsequent analysis.

First, for a signal $X_i \in \mathbb{R}^{n \times 1}$ in $\mathbf{X}$, where $i \in 1, \ldots, h$, we compute the Fourier transform $X_i(f)$ at each frequency band $f, f \in 1, \ldots, q$. The Magnitude Squared Coherence (MSC) [35] between signals from channels i and j, denoted as X_i and X_j, at frequency f is then computed using the following formula:

$$C_{ij}(f) = \frac{|S_{ij}(f)|^2}{S_{ii}(f) \cdot S_{jj}(f)}, \tag{1}$$

where $S_{ij}(f)$ is the cross-spectral density between X_i and X_j at frequency f, and $S_{ii}(f)$ and $S_{jj}(f)$ are the power spectral densities of X_i and X_j, respectively. They are defined as:

$$S_{ab}(f) = \mathbb{E}\left[X_a(f) X_b^*(f)\right], \quad a, b \in \{1, \ldots, n\} \tag{2}$$

where $X_a(f)$ and $X_b(f)$ are the Fourier transforms of X_a and X_b, respectively, and the asterisk (*) indicates the complex conjugate of the Fourier transform.

For each pair of channels, MSC is computed across all q frequency bands. The result is a pairwise coherence matrix $\mathbf{C} \in \mathbb{R}^{p \times q}$, where $p = h \cdot (h-1)/2$. Each entry $C_k(f)$ in $\mathbf{C}$ represents the coherence value, i.e., the MSC value, for the k-th pair of channels at frequency f, where $k \in \{1, \ldots, p\}$.

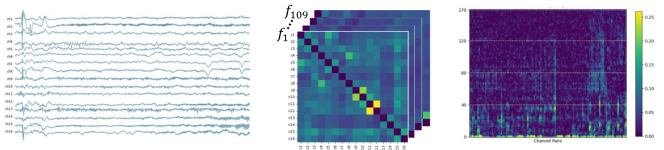

Fig. 3. An illustration of the coherence calculation in CoSP. (a) The raw EEG signal of a 10-second segment with 4000 time steps and 16 channels. (b) Coherence heatmaps for discretized frequencies from 0.5 Hz to 170 Hz. Each heatmap corresponds to a specific frequency, where each cell depicts the MSC between channel pairs at that frequency, with the color intensity indicating the level of coherence. The heatmaps are symmetric with diagonal cells omitted to represent self-coherence as 1. (c) A two-dimensional matrix stores the coherence values across different frequency bands, with 120 channel pairs on the x-axis and 109 frequencies on the y-axis. The color of each point indicates the MSC magnitude.

The matrix $\mathbf{C}$ serves as the input for the subsequent preictal probability estimation module.

Fig. 3 presents an illustrative example of transforming a 10-second EEG segment in the NeuroVista dataset into the pairwise coherence matrix as described above. The number of time steps, n, is 4000, corresponding to a sampling rate of 400 Hz. The segment comprises 16 channels, i.e., $h = 16$, resulting in 120 channel pairs, i.e., $p = 15 \times 16/2 = 120$. The frequency spectrum, which ranges from 0.5 Hz to 170 Hz, was discretized at intervals of 1.6 Hz, yielding a total of 109 discrete frequencies, i.e., $q = 109$.

2) Preictal Probability Estimation: The preictal probability estimation module employs a CNN to predict the probability of an 10-second EEG segment being preictal. As shown in Fig. 1 the CNN architecture consists of four convolutional blocks. Each block includes batch normalization to standardize inputs, a convolutional layer with ReLU activation for nonlinear processing, and a max pooling layer to reduce spatial dimensions. The convolutional sequence begins with 32 kernels of size 7x7, followed by 64 kernels of size 5x5, then 128 kernels, and finally 256 kernels, both of size 3x3. All blocks use a stride of 1 and perform max pooling over a 2x2 area.

When applying the CNN to the NeuroVista dataset, the input is the coherence matrix $\mathbf{C}$ with the dimension of 120×109, with output dimensions of the convolutional blocks being 60×54, 30×27, 15×15, and 7×6, respectively. After the convolutional layers, the output is flattened and passed through a fully connected layer with 128 units, batch normalization, ReLU activation, and a dropout rate of 50% to prevent overfitting. The final fully connected layer outputs the preictal probability of the EEG segment, denoted as ρ.

In the model training, class imbalance is a challenge due to the much longer interictal periods compared to the preictal periods. To address this, we down-sampled the interictal segments and up-sampled the preictal segments. For interictal sampling, we first identified specific days as the interictal interval preceding the preictal period. During this interval, we selected the first 10-second segment from every 10 minutes of EEG recordings. For the preictal segments, we created overlapping samples by taking 10-seconds segment at calculated time step intervals, and the interval was calculated to ensure that the number of preictal segments matched the count of interictal segments. To maintain training efficiency, a cap of 18,000 training segments was imposed when the total exceeded this number. The model was trained using the Adam optimizer with a learning rate of 1×10^{-5} and binary cross-entropy as the loss function. In the testing phase, 10-second interictal and preictal segments were sampled without overlap throughout the entire duration of the interictal and preictal periods.

3) Seizure Warning: Following a commonly used approach in previous studies [4], [39], [42], the seizure warning module processes the predicted probabilities from the probability estimation module to generate seizure warnings. Two critical parameters for developing and evaluating seizure warning systems are the Seizure Occurrence Period (SOP) and the Seizure Prediction Horizon (SPH). The SPH provides patients with lead time to take preventive measures, such as administering medication or moving to a safe environment, before a seizure occurs. The SOP, on the other hand, represents the window during which a seizure is expected to happen. In CoSP, the SOP is set to match the length of the preictal intervals, while the SPH corresponds to the prediction reservation time, which is fixed at 1 minute as shown in Fig. 2.

To mitigate large variations in 10-second predictions, the warning module applies a moving window to the predicted probabilities of 10-second EEG segments with the window length equal to the SOP. The moving average accumulates the predicted outputs of multiple consecutive segments. This aggregation mechanism smooths out noisy predictions and reduces the likelihood of triggering warnings due to transient fluctuations in the predictions.

A warning is triggered when the averaged probability exceeds a predefined threshold. Once a warning is issued, the module transitions into a warning state, initiating a refractory period equal to the SOP length. During this refractory period, the module is disabled from generating additional warnings, even if another smoothed probability exceeds the threshold.

Following a common way [39], the warning module is retriggerable. If a probability exceeds the threshold while the patient remains in the warning state, the refractory period resets to start from the corresponding 10-second segment, which extends the warning state. In this design, an uninterrupted warning is treated as a single warning, regardless of its total duration. This mechanism helps prevent alarm fatigue by reducing excessive alerts within a short time frame.

The choice of the threshold to trigger a warning significantly impacts the performance of the warning module. Hence with CoSP, a grid search is performed to optimize this threshold, aiming to maximize a balanced performance metric known as the Performance Product (PP) (discussed in Section III-A). This optimization is conducted exclusively on the validation set, which contains data that chronologically precedes the test set, to prevent information leakage to the test stage.

III. Results

In this section, we first introduce the performance metrics used for evaluation. We then analyze the overall performance

of CoSP, followed by a comparative analysis against a chance predictor and baseline methods.

A. Performance Metrics

The performance metrics utilized in the study included Area Under the Receiver Operator Characteristic Curve (ROC AUC) [29], Seizure Sensitivity (SS) [4], [42], Time in Warning (TiW) [4], [42], False Positive Rate per hour (FPR/h) [42], and Performance Product (PP) [16]. Notably, ROC AUC is a *segment-level* metric, used to evaluate the performance of the preictal probability estimation module using the predicted probabilities of 10-second EEG segments. In contrast, SS, TiW, FPR/h, and PP are *seizure-level* metrics, designed to assess the overall performance of the CoSP model including the seizure warning module.

ROC AUC is a threshold-free metric that evaluates the performance of classification models by summarizing the trade-off between the True Positive Rate (TPR) and the False Positive Rate (FPR) across all possible thresholds. It is particularly robust to class imbalance because it considers the proportion of true positives and false positives relative to the total actual positives and negatives. An ROC AUC value close to 1.0 indicates excellent model performance, while a value of 0.5 suggests performance equivalent to random guessing.

SS, TiW, FPR/h, and PP are threshold-dependent metrics used to evaluate the performance of the CoSP model. SS measures the proportion of seizures that are correctly predicted, with a seizure considered successfully predicted if it occurs while the patient is in a warning state. TiW represents the percentage of time a patient remains in a warning state, calculated as the proportion of time spent in the warning state relative to the total test time. False Positive Rate per Hour (FPR/h) quantifies the average number of false warnings issued per hour. A warning is regarded as false if no seizure occurs during the warning period. SS reflects the sensitivity of the model, while TiW and FPR/h capture the specificity.

To assess the overall performance, the PP metric is utilized, providing a balanced measure of performance. The PP metric is defined as $PP = SS \times (1 - TiW)$, where higher values of SS (better seizure detection) combined with lower TiW (fewer false alarms) indicate better overall model performance. A PP value close to 1 signifies optimal performance, balancing high sensitivity and specificity.

B. Overall Performance of CoSP

In the experiments, the interictal period was set to 2 days prior to the preictal period. As the optimal preictal duration varies across individuals, we evaluated CoSP using preictal intervals of 4, 15, 30, 45, 60, 90, 120, 150, and 180 minutes. The results corresponding to the highest PP for each patient are reported in Table II.

From Table II, the ROC AUC values across all patients exceed 0.5, indicating that CoSP consistently outperforms random prediction at the segment level. Overall, the ROC AUC values range from 0.65 to 0.91, with a median of 0.76. However, a high ROC AUC does not necessarily translate to superior seizure-level performance. For instance, for Patient 11, CoSP achieves an ROC AUC of 0.91 but a PP of 0.63, whereas for Patient 1, despite a lower ROC AUC of 0.78, CoSP attains a higher PP of 0.68. This discrepancy arises because seizure-level performance is influenced not only by segment-level accuracy but also by the selection of the warning triggering threshold and the distribution of predicted probabilities across segments.

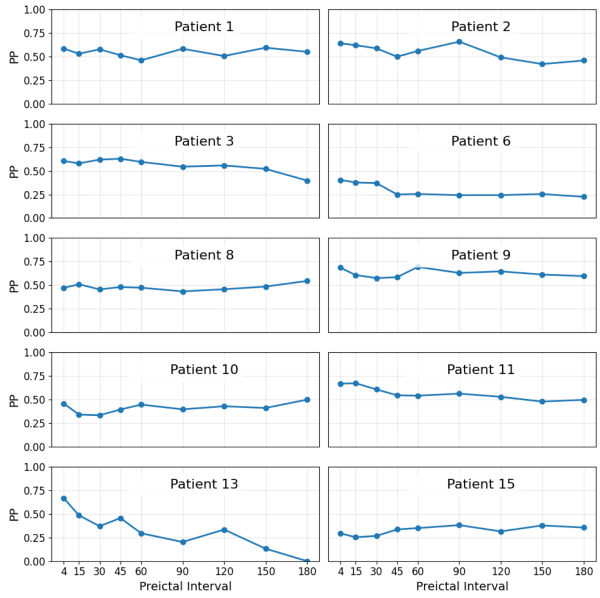

Fig. 4. PP values of CoSP models across different preictal interval lengths.

For seizure-level performance, SS ranges from 0.63 to 0.92, with a median of 0.79. FPR/h varies from 0.03 to 0.79, with a median of 0.15. TiW ranges from 12% to 35%, with a median of 27%. PP ranges from 0.44 to 0.69, with a median of 0.64. In summary, while CoSP achieves strong predictive performance, considerable inter-patient variability remains.

Additionally, as shown in Table II, the optimal preictal interval varies across patients. For some patients, such as patients 6, 11, and 13, CoSP demonstrated the best performance with very short preictal intervals of 4 minutes. In contrast, for patients 2 and 10, better results were achieved with longer preictal intervals of 90 and 180 minutes, respectively. The PP values across all preictal interval lengths is presented in Fig. 4, which shows that the selection of the preictal interval greatly impacts seizure prediction performance.

C. Comparison With the Baseline Methods

In this section, we compare CoSP with other seizure prediction methods applied to the NeuroVista dataset. Several studies have utilized the NeuroVista dataset for seizure prediction, including both non-deep learning methods [16], [17], [19], [28] and deep learning-based methods [2], [8], [12]. As CoSP is a deep learning-based approach, we compare it with all existing deep learning-based seizure prediction methods that used the NeuroVista dataset. Additionally, we also compare CoSP with two non-deep learning methods: the critical

TABLE III
PERFORMANCE COMPARISON OF COSP WITH OTHER STUDIES USING THE NEUROVISTA DATASET, PRESENTED IN THE FORMAT OF **SS/TIW/PP**

Patient	Critical Slowdown [16]	Deep CNN [12]	Original Trial [17]	CNN-LSTM [8]	LSTM [2]	Chance [39]	CoSP
1	**0.83/0.08/0.76**	0.65/0.21/0.51	0.77/0.27/0.56	0.84/0.15/0.65	0.83/0.42/0.48	0.69/0.66/0.24	0.92/0.25/0.68
2	**0.87/0.0002/0.87**	0.74/0.11/0.66	-	-	0.69/0.001/0.69	1.00/0.94/0.06	0.80/0.18/0.66
3	-	0.71/0.53/0.33	-	-	0.49/0.12/0.43	1.00/0.81/0.19	**0.91/0.29/0.65**
6	**0.66/0.03/0.64**	-	-	0.66/0.41/0.39	0.66/0.21/0.52	0.10/0.10/0.09	0.63/0.29/0.44
8	0.64/0.23/0.49	0.77/0.32/0.52	0.62/0.28/0.45	0.72/0.27/0.52	**0.78/0.20/0.62**	0.83/0.80/0.17	0.79/0.28/0.57
9	**0.85/0.16/0.71**	0.83/0.43/0.47	0.17/0.11/0.15	0.88/0.33/0.59	0.85/0.26/0.63	1.00/0.76/0.24	0.92/0.25/0.69
10	**0.78/0.24/0.59**	0.68/0.32/0.46	0.51/0.17/0.42	0.62/0.24/0.38	0.78/0.34/0.51	1.00/0.85/0.15	0.77/0.35/0.50
11	**0.86/0.16/0.72**	0.78/0.18/0.64	0.39/0.15/0.33	0.86/0.20/0.62	0.86/0.26/0.64	0.10/0.13/0.09	0.71/0.12/0.63
13	0.64/0.14/0.55	0.70/0.21/0.55	0.50/0.28/0.36	0.64/0.31/0.44	0.72/0.14/0.62	0.09/0.11/0.08	**0.79/0.16/0.67**
15	**0.87/0.001/0.87**	0.59/0.37/0.37	0.71/0.21/0.56	0.87/0.56/0.37	0.83/0.73/0.22	1.00/0.95/0.05	0.75/0.33/0.50
Significance	0.996	**0.009**	**0.015**	**0.004**	0.188	**0.001**	-

Methods with missing results are indicated by '-'. The statistical significance of the comparison between each method and CoSP, evaluated using the Wilcoxon signed-rank test, is shown in the p-value row.

slowdown model [16], considered the state-of-the-art (SOTA) on the NeuroVista dataset, and the machine learning approach from the original NeuroVista clinical trial [17], which serves as a baseline for comparison.

Among the deep learning-based methods compared, the Deep CNN model [12] applies a CNN to the spectrogram of EEG for seizure prediction. The CNN-LSTM model [8] combines LSTM and CNN to capture temporal changes in EEG features for improved prediction accuracy. The study by [2] explores using raw EEG data for seizure prediction. Notably, these methods incorporate time-of-day information to enhance prediction accuracy. Among the non-deep learning approaches, the original NeuroVista clinical trial [17] presents results utilizing an ensemble machine learning method for seizure prediction. The critical slowdown model [16] uses critical slowing down indicators and is considered the SOTA on the NeuroVista dataset.

Additionally, to verify whether CoSP performs above chance level, we implemented a chance predictor based on a Poisson process [39]. A seizure prediction model is considered to perform above chance if its results are statistically significantly better than random chance, with the significance level set to 0.05. This chance predictor operates independently of EEG signals, simulating a sensorless approach by generating preictal classifications uniformly across test time intervals.

The comparison results are presented in Table III, which shows that Critical Slowdown generally achieves the best performance across most patients, while CoSP also demonstrates strong performance for a majority of patients. To further evaluate the models, Wilcoxon signed-rank tests were conducted to compare the PP scores of CoSP with each baseline model and the chance predictor in a pairwise manner. These tests were designed to assess the hypothesis that CoSP outperforms the comparison methods. A p-value below 0.05 was considered statistically significant. CoSP performed significantly better than chance predictor, with a p-value of 0.001, and also outperformed Deep CNN, Original Trial, and CNN-LSTM, with p-values well below 0.05.

It is noted that although all models report SS and TiW, comparisons may not be entirely fair due to differences in evaluation configurations, such as segment-level vs. seizure-level analysis and variations in SOP lengths. The LSTM method uses segment-level predictions, while Deep CNN, Original Trial, and CNN-LSTM apply seizure-level evaluations with different SOP lengths. For Critical Slowdown, SS is seizure-level, but TiW's evaluation level is unclear.

IV. DISCUSSION

In this section, we present a case study to investigate why and how CoSP works. Using the results from Patient 13, we first analyze the coherence patterns in the iEEG data of Patient 13. Then, we explore how these patterns are captured and utilized by CoSP to make predictions, offering insights into the ability of CoSP to effectively differentiate between interictal and preictal states.

Analysis of Coherence Patterns. Coherence is a measure of synchronization, connection, and communication between brain regions. A high coherence value between two channels indicates a strong connection between the brain regions where the corresponding electrodes are located [37]. CoSP leverages coherence to predict seizures by analyzing the changes in these connectivity patterns.

Fig. 5 illustrates the top 15 strongest brain region connections, based on the average coherence values computed from the coherence matrices of 1,000 randomly selected interictal and preictal segments, respectively. These coherence values are averaged across six primary frequency bands: Delta (0–4 Hz), Theta (4–8 Hz), Alpha (8–12 Hz), Beta (12–30 Hz), Gamma Low (30–100 Hz), and Gamma High (100–170 Hz). The connections are visualized as lines overlaid on an X-ray of the patient's brain, showing the locations of the 16 electrodes. The color intensity of each line represents the magnitude of the coherence value, with stronger connections (i.e., higher coherence values) indicated by more intense colors.

Significant connectivity changes are observed in the Gamma High frequency band. In the interictal state, the connectivity network displays a somewhat clustered pattern around electrodes in the lower part of the X-ray, while maintaining scattered connections spanning different areas of the brain. In contrast, during the preictal state, the connectivity becomes highly focused and directional, with a clear convergence toward Electrode 1 (Channel 1), positioned on the far-right side of the X-ray. Lower frequency bands, on the other hand, exhibit relatively stable connectivity patterns between interictal and preictal states, showing fewer connectivity changes.

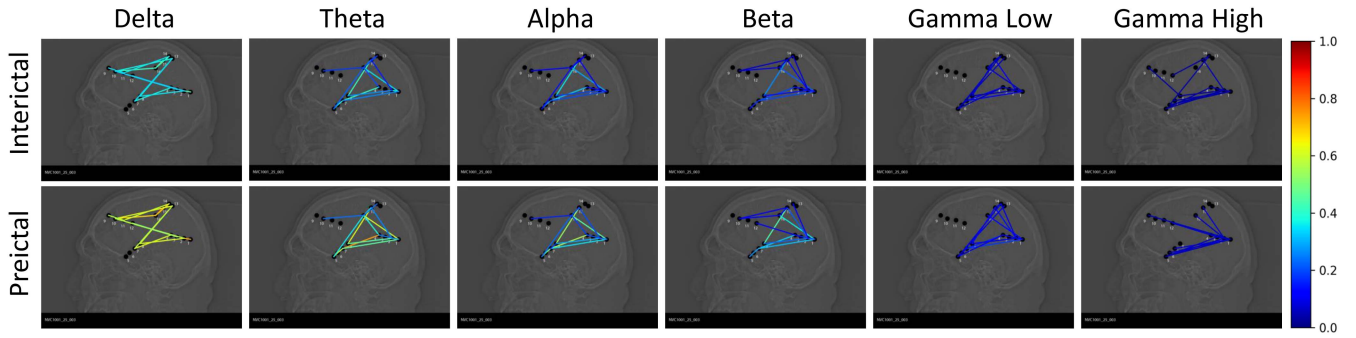

Fig. 5. Top 15 strongest brain region connections based on average coherence values computed from 1,000 randomly selected interictal and preictal segments across six frequency bands: Delta (0–4 Hz), Theta (4–8 Hz), Alpha (8–12 Hz), Beta (12–30 Hz), Gamma Low (30–100 Hz), and Gamma High (100–170 Hz). Significant changes are observed in the Gamma High band, where interictal connectivity is somewhat scattered and clustered in the lower brain regions, while preictal connectivity becomes strongly focused toward Electrode 1 (Channel 1) on the far-right side of the X-ray. Lower frequency bands show relatively stable connectivity patterns.

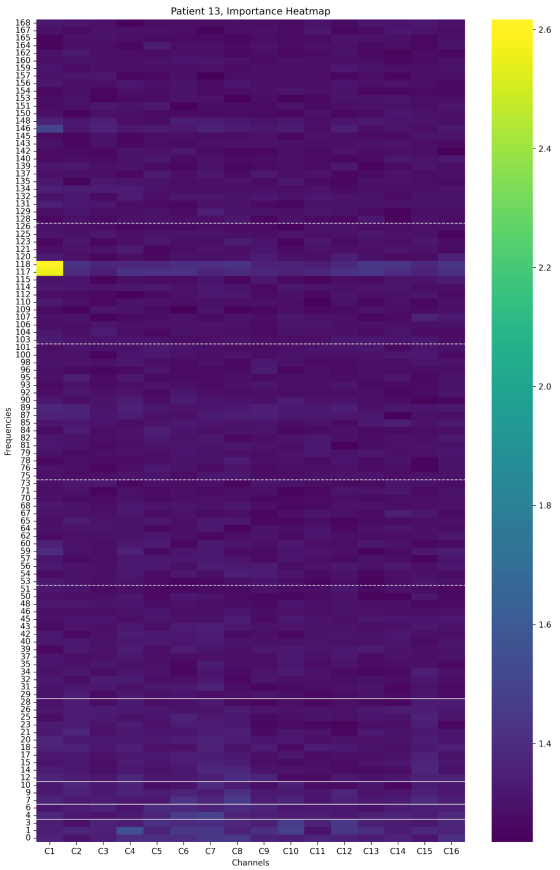

Fig. 6. Importance heatmap for CoSP predictions of Patient 13, explained using LIME. The heatmap visualizes the contributions of individual channels (C1–C16) and frequencies (0.5–170 Hz) to the predictions from CoSP. Brighter colors represent higher importance values. The heatmap reveals that Channel 1 (C1) at approximately 120 Hz holds the highest importance, aligning with the coherence patterns in Fig. 5.

How CoSP Captures Coherence Patterns for Prediction. To further investigate why CoSP is effective despite the lack of significant connectivity changes in most frequency bands, we applied Local Interpretable Model-Agnostic Explanations (LIME) [36] to analyze how CoSP makes predictions. LIME approximates complex models locally by fitting interpretable models, enabling the identification of the most influential features—channels and frequency bands—that contribute to the decision-making process of CoSP.

We applied LIME to interpret the 1,000 highest probability predictions and averaged the feature importance values to generate an importance heatmap, shown in Fig. 6. The heatmap reveals that Channel 1 (C1) at approximately 120 Hz holds the highest importance. This observation aligns with the coherence patterns in Fig. 5, where Channel 1 exhibited the most significant connectivity changes between interictal and preictal states in the Gamma High frequency band. The consistency between these findings confirms that CoSP effectively identifies and prioritizes the most relevant brain regions and frequencies for accurate seizure prediction.

Furthermore, this finding regarding Patient 13 aligns with prior research on high-frequency activity (HFA) in the NeuroVista dataset [3], [28], which reported that the iEEG data of Patient 13 exhibited significantly increased HFA in specific electrodes several minutes before seizure onset.

In summary, this case study has demonstrated that CoSP effectively captures subtle spatial and spectral changes across interictal and preictal states in pairwise channel coherence matrices, enabling accurate and reliable seizure prediction. Notably, these changes are complex, diverse, subtle, and highly patient-specific [3], [16], [28]. By leveraging deep learning, CoSP can automatically identify and learn these intricate patterns, highlighting the importance of utilizing full pairwise channel coherence information in conjunction with deep learning for robust and accurate seizure prediction.

V. Conclusion

In this study, we have presented CoSP, an innovative seizure prediction method that integrates full pairwise channel coherence with deep learning to capture subtle spatial and spectral changes in brain connectivity, thereby improving seizure prediction performance. Experimental evaluation using the long-term iEEG data of the NeuroVista dataset demonstrated that CoSP achieves high seizure sensitivity while maintaining reasonable

specificity across 10 patients. Statistical validation confirmed that CoSP significantly outperforms both chance predictor ($p = 0.001$) and baseline methods ($p < 0.05$) under similar evaluation configurations. Additionally, a detailed case study provided insights into why and how CoSP works, showcasing its ability to capture critical changes in brain connectivity before a seizure.

Future research could focus on incorporating temporal coherence patterns to analyze how brain connectivity evolves over time, potentially enhancing predictive performance. Additionally, integrating multiple biomarkers—such as auto-correlation, variance, spike rate, and seizure cycles—alongside coherence could contribute to the development of a more robust and clinically applicable seizure prediction system.

REFERENCES

[1] R. S. Fard, B. Abbaszadeh, and M. C. E. Yagoub, "Application of global coherence measure to characterize coordinated neural activity during frontal and temporal lobe epilepsy," in *Proc. 42nd Annu. Int. Conf. IEEE Eng. Med. Biol. Soc.*, 2020, pp. 3699–3702.

[2] J. D. Chambers, M. J. Cook, A. N. Burkitt, and D. B. Grayden, "Using long short-term memory (LSTM) recurrent neural networks to classify unprocessed eeg for seizure prediction," *Front. Neurosci.*, vol. 18, 2024, Art. no. 1472747.

[3] Z. Chen et al., "Spatiotemporal patterns of high-frequency activity (80–170 Hz) in long-term intracranial EEG," *Neurology*, vol. 96, no. 7, pp. e1070–e1081, 2021.

[4] H. Chenand and V. Cherkassky, "Performance metrics for online seizure prediction," *Neural Netw.*, vol. 128, pp. 22–32, 2020.

[5] R. Cooper, J. W. Osselton, and J. C. Shaw," *EEG Technology*. Berlin, Germany: Springer, 2014.

[6] EpiMinder, "Epiminder: Pioneering epilepsy management," 2024, Accessed: Jun. 20, 2024. [Online]. Available: https://epiminder.com/

[7] C. Li et al., "EEG-based seizure prediction via model uncertainty learning," *IEEE Trans. Neural Syst. Rehabil. Eng.*, vol. 31, pp. 180–191, 2022.

[8] D. E. Payne et al., "Epileptic seizure forecasting with long short-term memory (LSTM) neural networks," 2023, *arXiv-2309*.

[9] D. Lee et al., "A Resnet-LSTM hybrid model for predicting epileptic seizures using a pretrained model with supervised contrastive learning," *Sci. Rep.*, vol. 14, no. 1, 2024, Art. no. 1319.

[10] G. Wang et al., "Epileptic seizure detection based on partial directed coherence analysis," *IEEE J. Biomed. Health Inform.*, vol. 20, no. 3, pp. 873–879, May 2016.

[11] I. Ahmad et al., "EEG-based epileptic seizure detection via machine/deep learning approaches: A systematic review," *Comput Intell Neurosci*, vol. 2022, 2022, Art. no. 6486570.

[12] I. K. Kiral et al., "Epileptic seizure prediction using Big Data and deep learning: Toward a mobile system," *EBioMedicine*, vol. 27, pp. 103–111, 2018.

[13] J. West et al., "Machine learning seizure prediction: One problematic but accepted practice," *J. Neural Eng.*, vol. 20, no. 1, 2023, Art. no. 016008.

[14] K. M. Tsiouris et al., "A long short-term memory deep learning network for the prediction of epileptic seizures using EEG signals," *Comput. Biol. Med.*, vol. 99, pp. 24–37, 2018.

[15] K. Rasheed et al., "Machine learning for predicting epileptic seizures using EEG signals: A review," *IEEE Rev. Biomed. Eng.*, 14, pp. 139–155, 2020.

[16] M. I. Maturana et al., "Critical slowing down as a biomarker for seizure susceptibility," *Nature Commun.*, vol. 11, no. 1, 2020, Art. no. 2172.

[17] M. J. Cook et al., "Prediction of seizure likelihood with a long-term, implanted seizure advisory system in patients with drug-resistant epilepsy: A first-in-man study," *Lancet Neurol.*, vol. 12, no. 6, pp. 563–571, 2013.

[18] P. Boonyakitanont et al., "A review of feature extraction and performance evaluation in epileptic seizure detection using EEG," *Biomed. Signal Pessing Control*, vol. 57, 2020, Art. no. 101702.

[19] P. J. Karoly et al., "The circadian profile of epilepsy improves seizure forecasting," *Brain*, 140, no. 8, pp. 2169–2182, 2017.

[20] R. Shriram et al., "Energy distribution and coherence-based changes in normal and epileptic electroencephalogram," in *Title of the Book or Conference Proceedings*, Singapore: Springer, 2019, pp. 625–635.

[21] S. M. Usman et al., "Using scalp EEG and intracranial EEG signals for predicting epileptic seizures: Review of available methodologies," *Seizure*, vol. 71, pp. 258–269, 2024.

[22] U. R. Acharya et al., "Automated EEG analysis of epilepsy: A review," *Knowl.-Based Syst.*, vol. 45, pp. 147–165, 2013.

[23] V. L. Towle et al., *Electrocorticographic Coherence Patterns of Epileptic Seizures*. Berlin, Germany: Springer, 2003, pp. 69–81.

[24] Y. Li et al., "Spatio-temporal-spectral hierarchical graph convolutional network with semisupervised active learning for patient-specific seizure prediction," *IEEE Trans. Cybern.*, vol. 52, no. 11, pp. 12189–12204, Nov. 2022.

[25] Y. Roy et al., "Deep learning-based electroencephalography analysis: A systematic review," *J. Neural Eng.*, vol. 16, no. 5, 2019, Art. no. 051001.

[26] Y. Zhao, C. Li, X. Liu, R. Qian, R. Song, and X. Chen, "Patient-specific seizure prediction via adder network and supervised contrastive learning," *IEEE Trans. Neural Syst. Rehabil. Eng.*, vol. 30, pp. 1536–1547, 2022.

[27] Z. Chen et al., "High-frequency oscillations in epilepsy: What have we learned and what needs to be addressed," *Neurol.*, vol. 96, no. 9, pp. 439–448, 2021.

[28] Z. Chen et al., "Seizure forecasting by high-frequency activity (80–170 Hz) in long-term continuous intracranial Eeg recordings," *Neurol.*, vol. 99, no. 4, pp. e364–e375, 2022.

[29] J. A. Hanley and B. J. McNeil, "The meaning and use of the area under a receiver operating characteristic curve," *Radiol.*, vol. 143, no. 1, pp. 29–36, 1982.

[30] A. Harris and J. A. Gordon, "Long-range neural synchrony in behavior," *Annu. Rev. Neurosci.*, vol. 38, pp. 171–194, 2015.

[31] R. Hartanto, I. Wijayanto, and H. A. Nugroho, "Quantitative analysis of inter- and intrahemispheric coherence on epileptic electroencephalography signal," *J. Med. Signals Sensors*, vol. 12, no. 2, pp. 145–154.

[32] "International league against epilepsy," 2019, Accessed: Jun. 20, 2024. [Online]. Available: www.ilae.org

[33] T. A. Pedley, J. Engel, and J. Aicardi, *Epilepsy: A Comprehensive Textbook*. Philadelphia, PA, USA: Lippincott Williams & Wilkins, 2008.

[34] S. Shelagh, "EEG in the diagnosis, classification, and management of patients with epilepsy," *J. Neurol. Neurosurgery Psychiatry*, vol. 76, no. suppl 2, pp. ii2–ii7, 2005.

[35] J. G. Proakis. *Digital Signal Processing: Principles, Algorithms, and Applications*. Noida, India: Pearson Education India, 2007.

[36] M. T. Ribeiro, S. Singh, and C. Guestrin, ""Why should I trust you?" explaining the predictions of any classifier," in *Proc. 22nd ACM SIGKDD Int. Conf. Knowl. Discov. Data Mining*, 2016, pp. 1135–1144.

[37] B. Schelter, M. Winterhalder, J. Timmer, and J. Kurths, "Phase synchronization and coherence analysis: Sensitivity and specificity," *Int. J. Bifurcation Chaos*, vol. 17, no. 10, pp. 3551–3556, 2007.

[38] J. C. Shaw, "Correlation and coherence analysis of the EEG: A selective tutorial review," *Int. J. Psychophysiol.*, vol. 1, no. 3, pp. 255–266, 1984.

[39] D. E. Snyder et al., "The statistics of a practical seizure warning system," *J. Neural Eng.*, vol. 5, no. 4, pp. 392–401, 2008.

[40] C. E. Stafstrom and L. Carmant, "Seizures and epilepsy: An overview for neuroscientists," *Cold Spring Harbor Perspectives Med.*, vol. 5, no. 6, 2015, Art. no. a022426.

[41] S. Weiss and H. M. Mueller, "The contribution of EEG coherence to the investigation of language," *Brain Lang.*, vol. 85, no. 2, pp. 325–343, 2003.

[42] M. Winterhalder, T. Maiwald, H. U. Voss, R. Aschenbrenner-Scheibe, J. Timmer, and A. Schulze-Bonhage, "The seizure prediction characteristic: A general framework to assess and compare seizure prediction methods," *Epilepsy Behav.*, vol. 4, no. 3, pp. 318–325, 2003.